

Assessment of deep aquifer development and its implications in granitic terrain using isotopes and chemistry

Venkat D Reddy (✉ dvreddy.ngri@gmail.com)

National Geophysical Research Institute <https://orcid.org/0000-0001-8926-7868>

Devender Kumar

NGRI: National Geophysical Research Institute CSIR

B. Kiran Kumar

NGRI: National Geophysical Research Institute CSIR

S. Kiran Kumar Reddy

NGRI: National Geophysical Research Institute CSIR

D. Shashidhar

NGRI: National Geophysical Research Institute CSIR

Research Article

Keywords: paleo-groundwater, deep aquifer, blind/discrete sheet joints, stable isotopes, hydrochemistry, aquifer inter-connection

Posted Date: March 22nd, 2022

DOI: <https://doi.org/10.21203/rs.3.rs-1323380/v1>

License: © ⓘ This work is licensed under a Creative Commons Attribution 4.0 International License. [Read Full License](#)

Abstract

This study is conducted in the Precambrian granitic terrain, to demonstrate the presence of the multi-aquifer system and examine the inter-communications between them. Distinct hydrochemical characters of the groundwater from shallow (~ 100 m) and deep (~ 400 m) wells, signifies their independent and unconnected nature initially. Hydrochemistry of deep groundwater is approximately constant (either Ca-Na-Cl or Ca-Na-Cl-SO₄ type of water) during January 2015 to June 2016. Repeated carbon-14 measurements during the same period show the ¹⁴C activity of about 35 to 85 pMC (residence time about 3 to 8 ky BP). However, as a result of excess rainfall during 2016, hydrochemical facies of deep groundwater changed initially to Na-Ca-SO₄-Cl and subsequently stabilised at Ca-Na-HCO₃-Cl type with a drastic reduction in Cl and increased HCO₃ and NO₃ concentrations, while the ¹⁴C activity turned out to be to 100 pMC (modern age). These changes are attributed to ingress of fresh water into the deep aquifer, after paleo-groundwater depleted due to prolonged drought conditions along with the over-exploitation of limited potential deep aquifer. These drought and over-exploitation situations potentially improved the migration potential of fresh water to the deep aquifer and led to enhancing the groundwater recharge during the excess rainfall years. This brings a new perspective to the hydrogeological dynamics between shallow and deep groundwater. A conceptual model is proposed to explain the observed phenomenon. This study also suggests that, under climate driven drought conditions, deep aquifers could act as emergent groundwater resource to meet the water demands amid population growth.

Introduction

The occurrence and flow of groundwater is a complex phenomenon in the hard rock terrain (Ayraud et al., 2008, Gleeson et al., 2009, Guihéneuf et al. 2014, Ofterdinger et al. 2019). In hard rock terrains, usually the groundwater availability is restricted to the weathered and fractured zones primarily under phreatic conditions, though at times, it occurs under semi-confined conditions too. The hard rock aquifers are considered as two-layer system in which the weathered zone below the ground surface act as capacitive layer and the fractured layer underneath, act as transmissive layer (Durand et al., 2017). Normally, the fracture system in the granitic rocks is vertical or inclined, however, horizontal or curved sheet joints are also common (Jahns, 1943, Maheshwari et al., 2013, Guihéneuf et al. 2014). Erratic rainfall and frequent droughts often lead to over-exploitation of shallow aquifers, particularly in semi-arid hard rock regions (Reddy et al., 2009, de Graaf et al., 2019). This leads to severe water crisis due to limited groundwater potential in the shallow aquifers in these regions (CGWB, 2011). In order to meet the water demand, exploration and exploitation of deep aquifers is gaining movement (Chandra et al., 2012, 2019), in highly populated countries like India. However, the groundwater potential of deep aquifers mainly depends on the interconnectivity of the fracture system (Sukhija et al., 2006, Chandra et al., 2019, Collins, et al., 2020), and hence, understanding this phenomenon is essential, especially in the hard rock regions, where groundwater potential is low.

The sheet joints often develop due to release of overburden stress in granitic terrains (Cook, 2003) or because of the compressional stresses (Martel, 2017, Stephen, 2017). They are typically horizontal or curved, mimicking the surface topography and can have dimensions up to few hundreds of meters (Matthes, 1930, Holzhausen, 1977, Bahat et al., 1995). The studies on sheet joints in New England indicated their lengthening with increasing depth below the surface (Jahns, 1943). Most of the groundwater conceptual models in hard rock regions proposed so far by different researchers deal with weathered and fractured zones and their interconnection (Dewandal et al., 2006, Gleeson et al., 2009, Collins et al., 2020), while the role of sheet joints and their connectivity has not found prominence. Generally, at shallow depths, these sheet joints crosscut with the vertical fractures/joints but may remain as blind fractures when formed at deeper depths (Singhal and Gupta, 1999). Recharging of water in these blind and deep sheet joints takes place typically through the surrounding minor/major cracks and water may permanently resides in such sheet joints, however, they may act as dry fractures at times. Scanty literature reports about such blind fractures in context with groundwater makes it important to study the deep aquifer system apropos its potential and sustainability. Studies on interconnectivity of shallow and deep aquifers will be helpful for better understanding of the recharge mechanisms and their sustainability in the hard rock terrains.

The present work aims to understand the deep aquifers and their induced communication with the shallow aquifers in the hard-rock terrain under varying climatic conditions. Hydrochemical and isotopic characterization of surface and groundwater have been used to distinguish the shallow and deep aquifers. The influence of drought conditions on shallow and deep aquifer system and their interconnectivity have been assessed. A conceptual model is proposed to understand the fast recharge conditions to deep aquifer due to induced communication by depicting the study area conditions when such aquifer is over-exploited.

Study area

The present study is carried out in the Neredmet area situated in the northern fringes of the Hyderabad city in India (Fig. 1a). The rapid urban growth since 1989, has led to many economic, social and environmental problems, simultaneously stressing the available groundwater resources (Wakode et al., 2014). The region is covered with hard compact Precambrian granitic terrain of Peninsular Gneissic Complex (PGC). Topographic elevation of the study area is about 555 m above mean sea level (msl). Eastern and western sides of the study area are covered with rocky hillocks of ~ 40 to 50 m high, makes like a little valley in the central portion, slopping locally and regionally towards south (Fig. 1a).

In the western part of the study area, an open granite quarry (Fig. 1b) of about 3-4 m deep with reference to the present surrounding ground surface. Few domes like rocky portions left in the central part of the quarry indicate limited sets of fracture system in the massive granite. On the eastern edge of the quarry, a few east dipping sheet joints are observed. During rainy season the quarry is filled with rainwater for a short period by creating a surface water body of ~ 0.065 km² (maximum water spread area). Due to existing sheet joints, this surface water body may act as one of the water sources for the phreatic aquifer in the study area. Comparatively larger Kapra lake (~ 0.350 km²), located about 2.5 km away in the NE direction, belongs to another drainage system flowing

towards south-west. Another surface reservoir (Ramakrishnapuram lake, $\sim 0.170 \text{ km}^2$) is located approximately one km away in the down gradient (southern side) (Fig. 1a). Thus, the groundwater system in the study area has meagre chances to get any contribution from these two lakes.

Before 2005, the area was practically barren land. Thenceforth, the construction of multi-storeyed apartments (high-rise dwellings) started and peaked around 2010. Lack of Municipal water-supply and demand for construction work, domestic needs and drinking water, forced every individual house to drill their own borewells up to the depth of about 100 m. Increased construction activity led to enhanced groundwater exploitation to cater the domestic and new construction needs. This excess withdrawal of groundwater in association with draught conditions, resulted in a very fast depletion of phreatic aquifers. Thereby, in search of water, led to drilling of new deep wells to $\sim 400 \text{ m}$, where the groundwater potential zone was encountered.

Shivam-1 and Shivam-2 apartments (constructed in 2007-08), initially had 2 shallow bore wells ($\sim 100 \text{ m}$) used for the construction activity and later for domestic purpose. When these shallow wells dried up during the low rainfall years (2012 and 2013), two new deep ($\sim 400 \text{ m}$) bore wells (D1 and D2, $\sim 50 \text{ m}$ apart) were drilled during October and November 2014 in respective apartments (Fig. 1b). D1 and D2 wells encountered a potential aquifer at a depth of $\sim 366 \text{ m}$ after crossing the compact rock. In another apartment Yashokiran (located opposite to Shivam-2, constructed in 2005), existing 122 m bore well went dry in 2014 and was deepened up to 390 m (D3) during December 2015. The distance between D2 and D3 is only $\sim 20 \text{ m}$ (Fig. 1b). Subsequently, knowledge of groundwater potential zone at $\sim 400 \text{ m}$ led people of the new and old housing complexes in the surrounding area to drill their wells up to 400 m or deeper. However, northern part of the study area, which is relatively higher topography, covered with independent houses of one or two floors are still being served with the shallow bore wells ($\sim 100 \text{ m}$ depth) till now for their domestic needs. As per the general practice in hard-rock area, all the bore wells are open (no casing) except top 5 to 10 m casing (depending upon the weathered zone thickness). Hence, while pumping, groundwater mixing takes place depending upon the number of water yielding fractures encountered in the well.

Rainfall

Annual average rainfall of Hyderabad is $\sim 850 \text{ mm}$ (Fig. 2a) and $\sim 75\%$ of it comes from the South West (SW) monsoon during June to September (Fig. 2b). Besides, substantial rainfall occurs during October to January due to the North East (NE) monsoon. From February to May (summer months), $\sim 5\text{-}10\%$ of rainfall occurs due to cyclonic events. Daily distribution of rainfall for the years 2015 to 2017 is shown in Figure 2c (data source, Indian Meteorological Department).

The rainfall data of the period 2005 to 2018 (representing the start of the construction activity in 2005) is analyzed for this study. During this period, 7 years received more than normal and the other 7 years received subnormal rainfall. The low rainfall years i.e., 2011 (625 mm) and 2012 (778 mm) were followed by high rainfall in 2013 (1089 mm). However, again 2014 (608 mm) and 2015 (530 mm) were low rainfall (drought) years. 2015 being the lowest rainfall year, one cyclonic event on 13/4/2015 delivered $\sim 10\%$ of the annual rainfall. Subsequent years, 2016 and 2017 received high rainfall i.e., 1014 and 1025 mm respectively (Fig. 2a).

Methods

Groundwater sample collection

A total of 56 groundwater samples were collected from January 2015 to August 2019 from the 9 bore wells of depth ranging from 61 to 410 m for hydrochemical and stable isotope measurements. All the sampled wells are being used for domestic purpose and sampling was made in pumping condition. The sampled wells are categorized as shallow (S) (depth ranging from 61 to 107 m) and deep (D) (depth $\sim 400 \text{ m}$) wells. Samples from four shallow (S1 to S4) and two deep wells (D4 and D5) were collected only once (during April 2015). Repeated sampling was carried out from the 3 deep wells (D1, D2 and D3) from 2015 to 2019 (Table 1). Distribution of sampled deep wells is clustered in the southern side, while the shallow wells are located in the northern part (Fig. 1b). One sample from the granite quarry located $\sim 300 \text{ m}$ west of D1, was collected on 30-08-2019, almost at the end of SW monsoon period, when water was available only in the deepest portion of the quarry pits.

For carbon-14 (^{14}C) measurement, first sampling was carried out in D1 and D2 wells in February 2015 and was repeated 6 times until December 2016. D3 was sampled 5 times between May 2015 and December 2016. The last collection was made from all these 3 wells in August 2019 (Table 1). Considering the low bicarbonate content in groundwater, for the first four collections, 200 to 400 liters of sample was collected, however, afterwards it was only 50 to 100 liters as a result of increased bicarbonate concentrations which yielded sufficient carbon dioxide for dating purpose.

Hydrochemical measurements

Physico-chemical parameters like pH, Eh, electrical conductivity (EC) and total dissolved solids (TDS) were measured in-situ with a portable "Consort" multi-parameter analyzer. The concentration of the bicarbonate (HCO_3) and carbonate (CO_3) were determined in the laboratory using standard titration method on the day of collection. Major ion concentrations of the anions like fluoride (F), chloride (Cl), nitrate (NO_3), and sulphate (SO_4) were analysed with an AS-14 column and that of the cations like sodium (Na), potassium (K), calcium (Ca), magnesium (Mg) with a CS-17 column using the Ion Chromatography systems (Dionex® IC-90 and IC-2500). Before measuring the actual samples, everyday four standards (mixture of anions/cations) with different concentrations (procured from Merck®) were used, where the linearity is >0.99 . The analytical precision of the instrument is $\sim \pm 1\%$ within the run and $\sim \pm 5\%$ between different runs. Ionic charge balance of the majority of the samples is within 5%. The $\delta^{18}\text{O}$ and δD values were determined with a dual-inlet stable isotope ratio mass spectrometer (IRMS, Isoprime®) referring to the Vienna Standard Mean Ocean Water (VSMOW). The precision is $\pm 0.1\text{‰}$ and 1‰ for $\delta^{18}\text{O}$ and δD respectively. Hydrochemical and isotopic measurements were made in our laboratory at CSIR-NGRI. Stable isotopes ($\delta^{18}\text{O}$ and δD) measured on

33 rainwater samples (rainy days) collected at CSIR-NGRI automatic weather station during 2010 are used for this study. Yearly rainfall at this weather station in 2010 agrees well with Hyderabad rainfall in the same year.

^{14}C measurements were made at CSIR-NGRI with a low-level liquid scintillation counter (Quantulus®). The sample processing and measurement protocols are followed as reported by Sukhija et al. (2006) and Gupta and Polach (1985). Considering the problems and limitations of ^{14}C dating of groundwater samples (IAEA, 2013, Ian Cartwright et al 2020, Liang-Feng Han et al., 2021), ^{14}C activity is reported here as percent modern carbon (pMC) and uncorrected ^{14}C dates given in the bracket as well as in the Table 3 are only indicative.

Results And Discussions

Groundwater status in and around Study area

The domestic usage of the studied bore wells precludes to measure the groundwater levels in those wells. Hence, the data from nearest observation well at Malkajgiri village (~ 3 km south of the study area) monitored by State Groundwater Board, Telangana, has been used to get the best assessment of hydrodynamic conditions in the study area. Monthly groundwater levels measured in this piezometer of about 30 m deep are presented in figure 3 from 2005 to 2018 along with the monthly rainfall data. Seasonal groundwater level fluctuations in the observation well shows, in general between 10 to 15 m in various normal/above normal rainfall years, whereas < 5 m during the drought (2011 to 2015) period, with an overall drop in groundwater level of about 5 m between 2005 and 2018. 2011 being below normal rainfall year the raise in groundwater level between pre and post monsoon is only about 3 m, and further, the drought effect on groundwater system during pre-monsoon of 2012 is clearly seen, where the groundwater levels dropped down to 25 m (Fig. 3). The groundwater levels remained at about 25 m bgl till pre-monsoon 2016 with little monsoonal fluctuations. The drought effect on groundwater system is observed not only in the study area, but also entire Telangana state (CGWB, 2016). The drop-in groundwater level is highest in the Medak district in which the study area is located. During this period, most of the dug wells and the shallow wells had gone dry, indicating the desaturated phreatic aquifers. To meet the water demand, several deep bore wells were drilled in the study area, as well as in the Telangana State.

In the study area, the D1, D2 and D3 wells drilled during the severe drought period (2014-15) and started extraction from the deep aquifer. As these wells are being used for domestic purpose and quite deep, it is not possible to measure the groundwater levels.

Hydrochemistry

Based on the physico-chemical analysis of 57 (56 groundwater and one surface water) samples collected from the study area, statistical distribution of different ions is given in Table 2 while Table -3 shows the total data. A large variation is observed in almost all the ionic concentrations of shallow and deep well waters (Table 2) as well as a large variation within the deep well water chemistry.

For the four shallow well waters, the pH is less than 7, and the TDS ranges from 502 to 840 mg/L. The Ca and HCO_3 concentrations are more than twice of the Na and Cl concentrations respectively. High NO_3 concentrations ranging from 32 to 125 mg/l are found in all the 4 shallow well samples. In comparison to shallow groundwater samples, the single surface water sample from the granite quarry shows very high TDS (3108 mg/L), could be due to enrichment of ions owing to evaporation as the sample collected when only little water left in the quarry.

For the deep bore wells, the average pH value (~ 7.5) tends towards alkaline while the TDS ranges from 959 to 1862 mg/L. To study the temporal variations of different ions in deep wells, D1, D2 and D3 are sampled many times, whereas D4 and D5 were sampled only once along with other three deep wells in April 2015. Hydrochemistry of all these 5 wells is almost the same, as these wells encountered the same aquifer and are situated in close proximity. However, a large temporal variation is found in the hydrochemistry of deep well waters (Fig 4 of D1, D3 and D4 shown in Supplementary Information as SI-1 and 2). For these three deep wells, the dominating Cl ion from 2015 to first half of 2016 decreased sharply during the second half of 2016, whereas, the HCO_3 increased. In D1, Na and Ca concentrations are almost same (~300 mg/l) during 2015 and first half of 2016 (Fig. 4), and later, both the ions decreased to less than half. However, water chemistry of D2 and D3 is observed to be slightly different from that of D1. During the first half of 2015, D2 and D3 show relatively lower Na and Ca (SI-1 and 2) than D1, while from second half of 2015 to first half of 2016, their Na and Ca concentrations are almost similar to that of D1. Subsequently, concentrations of all chemical parameters in waters of there 3 wells drastically decreased, whereas HCO_3 and NO_3 increased. Before September 2016, there were only traces of NO_3 (except in April 2015) in all the 3 well waters, its concentration increased considerably afterwards.

Hydrochemical facies variations

Hydrochemical facies variation between the shallow and deep groundwater and the temporal changes in the deep groundwater are shown in the piper diagram (Fig. 5). Four shallow groundwater samples (S1 to S4) are mixed type, wherein 3 (except S1) samples have Ca and HCO_3 ions dominating the others indicating the freshly recharged groundwater (Ray and Mukherjee, 2008, Reddy et al., 2009). In S1 well, Ca and Na concentrations are almost equal but slightly differ from those in other 3 samples (S2 to S4) indicating a little ionic exchange. Deep waters from wells D1, D2 and D3 collected during January 2015 to June 2016 (12 samples from each well) and D4 and D5 (one-time collection) are either Ca-Na-Cl or Ca-Na-Cl- SO_4 type (Table 3, except one sampling of D1) considered as paleo-waters (Fig. 5). The sample from D1 collected on 16-04-2015 show Ca-Na-Cl- HCO_3 type (Table 3). Sudden drop in Na, Cl and SO_4 and increase in HCO_3 changing the water type from Ca-Na-Cl to Ca-Na-Cl- HCO_3 , indicates mixing of fresh water. Though sampling was made from wells D1 and D2 merely a day after summer rain storm (on 16-4-2015), only D1 indicate fresh water mixing. In September 2016, D1 and D2 water type changed to Ca-Na- SO_4 -Cl with increased SO_4 concentration and decrease in that of Cl. Further samplings between December 2016 to August 2019, HCO_3 concentration increased while that

of Cl and SO₄ decreased in all the 3 deep well waters. This change in water quality (Fig. 5) indicates mixing or replacement of fresh water with paleo-water. Single quarry sample indicated mixed water type (Na-Ca-K-Cl-SO₄).

Temporal variation of ¹⁴C activity and stable isotopes in groundwater

¹⁴C activity in the deep groundwater

¹⁴C activity measured in twenty samples from three deep well waters (D1 to D3) for the period 2015 to 2019 varies from as low as 35.41±0.48 pMC (uncorrected age of 8510±110 y BP) to 100 pMC (Modern, defined as 95% of the ¹⁴C activity for AD 1950, Stuiver and Pollach, 1977) (Fig. 6a, Table 3). For the first sampling, long residence time (time spent in the aquifer or time with reference to recharge, lowest pMC) is observed for the D1 sample (35.41 pMC (8510±110 y BP), followed by D2 (66.62 pMC, 3360±83 y BP) and relatively short residence time for D3 (85.01±0.8 pMC, 1340±78 y BP). This difference in pMC may be due to mixing of some water from other sheet joints (Cook et al., 2005). Fairly large fluctuations are observed in the ¹⁴C activity of the waters sampled from 2015 to mid-2016, wherein D1 and D3 show different pattern than D2. Since December 2016, all the water samples yielded “100 pMC” indicating fresh water influx into the aquifer. Change in ¹⁴C ages in deeper aquifer water is the result of mixing with shallow water (Takahashi et al., 2013). A good correlation is found between the HCO₃ concentration and the ¹⁴C activity in the paleo-waters (Fig. 6b). However, mixing/replacement of fresh water perturbed the correlation, indicating the fresh water ingress in December 2016 sampling.

Temporal variation of stable isotopes in groundwater

Out of the four shallow well waters, S4 yielded depleted stable isotope values (δ¹⁸O -3.29 ‰ and δD -18.8 ‰), while the S2 and S3 waters show relatively enriched values δ¹⁸O (-1.7 to -1.0 ‰) and δD (-17 to -10 ‰). The well S1, located in the east of the quarry, shows highly enriched δ¹⁸O (8.28 ‰) and δD (27.69 ‰) values. As expected, the surface water sample from the granite quarry (an evaporative body) measured positive δ¹⁸O (2.04 ‰) and δD (7.77 ‰) values. Hence, the well S1, located on the down gradient of granite quarry, has expectedly maximum influence of quarry water and the S4 has minimum influence.

δ¹⁸O and δD values of majority of water samples from D1, D2 and D3 are around -2±0.5 ‰ and -17±2 ‰ respectively (Fig. 7, Table 3). However, the anomalous values are observed in all the three wells.

The local meteoric water line (LMWL: δD = 7.8713 * δ¹⁸O + 9.8933) drawn based on the rainwater data set of year 2010, is almost similar to Indian Meteoric Water Line (IMWL, δD = 7.93 * δ¹⁸O + 9.94, Kumar et al., 2010) as well as the global meteoric water line (GMWL: δD = 8 * δ¹⁸O +10: Craig, 1961). The δ¹⁸O vs δD plot (Fig. 7) for the groundwater samples from the study area shows linear relationship with a characteristic slope of 4.4 (δD = 4.4057* δ¹⁸O - 6.4356, R² = 0.9484), excluding the two sets of data (collected during 26-09-16 and 20-01-18) for the deep wells. Overall, the low slope value is indicative of the evaporation (He et al., 2012, Bahir et al., 2019). Stable isotope values (~ -2±0.5 ‰ of δ¹⁸O and ~ -17±2 ‰ of δD) of deep well waters with longer residence time, indicate fairly stable climatic conditions at the time of recharge (Roy et al., 2021). However, the enriched stable isotope values in the mixed water even after mixing of the recent water with paleo-waters certainly indicates that the source of this recent water has undergone evaporation. The single surface water sample from the quarry pond also fall on the evaporation line, indicating that this may be one of the prominent sources of the water mixing with the paleo-groundwater. Highly depleted δ¹⁸O and δD values for the 26-09-16 collection from D1 and D2 (Table 2) may be due to direct rainfall recharge through preferred pathways, where, few rainwater samples (during the August) also measured similar values. Probably, during this period, paleo-water in the deep aquifer might have totally exhausted and allowed the maximum fresh water input to the aquifer, changing the ¹⁴C activity to 100 pMC or ‘Modern’ (as indicated in December 2016 collection). The set of 3 deep samples (D1, D2, D3) collected on 20-01-18 indicate enrichment of the stable isotope values in different proportions, probably due to major contribution from an evaporative body.

Sources of recharge to shallow and deep aquifers

Broadly, the shallow and deep-water chemistry shows that, shallow waters are acidic type (pH <7) and deep waters are slightly alkaline type (pH ~7.5). Acidic type of water in shallow aquifer indicate direct rainfall recharge (generally, rainwater is acidic) either through direct percolation or through preferred pathways. Average TDS value of the shallow groundwater (656 mg/L) is less than half of the deep aquifer water (1381 mg/L), indicates that these two waters are different. The major ionic dominance in shallow water is HCO₃ > Cl > SO₂ and Ca > Na > Mg, whereas in the deep waters, it is Cl > SO₂ > HCO₃ and Na > Ca > Mg. Very high NO₃ concentrations are observed in the shallow waters, whereas in most of the deep-water collections it is low. F concentrations are almost the same in the shallow and deep waters.

The maximum permissible limit of NO₃ concentration in drinking water is 50 mg/l under WHO (2008) and 45 mg/L (BIS 2012) as per Indian guidelines and its concentration in groundwater is an indicator of anthropogenic pollution (Reddy et al., 2010, 2015, Wakode et al., 2014). The absence of drainage system for sewage in the study area compels individual house/apartments to have their own soak pits, which, generally are the sources of high NO₃ concentration in phreatic aquifers (Reddy et al., 2015, Sridevi et al., 2017). In the present case, shallow well waters have NO₃ concentrations measured between 30 to 125 mg/L. Deep groundwater (under confined like condition) from D1 to D5 wells yielded only <10 mg/L of NO₃ until mid-2016, except one sample from D1 in the beginning of 2015 rainy season (Fig. 4). However, NO₃ concentration increased many folds in the D1 to D3 wells water from September 2016 onwards (Figs. 4, and SI-1 and 2). The relation between Cl and NO₃ concentrations clearly shows 2 groups of water (Fig. 8), i.e, paleo-waters and the recent recharge. While there is no relation between Cl and NO₃ for paleo-waters, a good relation exists for recent recharge. Samples collected from shallow wells also falls in this group.

Sudden raise in groundwater and depletion of stable isotopes due to snow melt recharge has been attributed to extremely rapid and localized recharge to fractured rock aquifers (Gleeson et al., 2009). Sudden change in water chemistry (presence of high NO_3 , K, HCO_3 , Fig. 4) and enriched stable isotope values are observed for the collection of 16-04-2015 for D1 (a day after the summer rainstorm event). This data shows fast migration of fresh water from a evaporative surface water body through desaturated weathered/fractured zone and mixing with deep aquifer water. However, the hydrochemistry and stable isotope values regained to the previous values (prior to the rainstorm event) within a week (Fig. 4). It clearly indicates that the mixing of fresh water has influenced only a limited extent around the bore well and not the entire aquifer. This could be possible when fresh water entered through the well hole (like artificial recharge) connecting the shallow and deep aquifers. When the shallow aquifer thus got desaturated, the sheet joints in the quarry facilitated fast migration of the rainstorm water from the quarry to the shallow aquifer initially. Subsequently, the well holes (connecting the shallow aquifer and partially depressurized deep aquifer) provided the direct path for this fresh water (rainstorm water) to migrate from shallow to deep aquifer. Thus, the fresh water entered in to the deep aquifer through well hole, mixed with deep aquifer water mainly around the well and thereby, diluted the deep aquifer water. Further, subsequent pumping yielded less mineralized water for a short time, as indicated by the measurements of the water samples collected on 16-04-2015 (Fig. 4). Hence, the chemistry of pumped water changed back to the original concentration within a week (Fig. 4). April 2015 summer storm effect is minimal on D2 well, which is 50 m east of D1. Though sample could not be collected from the D3 well on 16-04-2015, lowering of certain ion concentrations observed in the sample collected on 22-05-15 (Fig. 5), indicates the influence of the fresh water mixing on this well.

Relatively lower ^{14}C activity (higher ages) in all the 3 deep wells for June 2016 collection indicate presence of the paleo-water (Fig. 6a) till that time when the shallow aquifer was dry and hence, no freshwater contribution to the deeper aquifer. Change in hydrochemistry for September and December 2016 collection and 100 pMC ^{14}C activity for December 2016 collection shows fresh water ingress into the deep aquifer. It may be inferred that excessive extraction from the limited potential deep aquifer during the drought conditions in 2015, desaturated it to a great extent and thus creating favorable conditions to receive more fresh water during the excess rainfall year 2016. Due to the heavy rainfall, initially it recharged the shallow aquifer and subsequently, the same migrated to deep aquifer through the 3 studied deep wells and probably through many other such deep wells existing in the surrounding area. The steep increase in HCO_3 and NO_3 and simultaneous drop of SO_4 and Cl provides credible evidence that young/fresh groundwater has refilled the sheet joints emptied by excess pumping. It is further confirmed by the hydrogeochemical measurements and ^{14}C activity of the 3 deep wells waters in August 2019 and stable isotope data (Table 2).

Conceptual hydrogeological model of the study area.

Occurrence of sheet joints in the granitic terrain is a common phenomenon (Maheshwari et al., 2013). Quite often, they intersect with vertical joints at shallow level (Devandal et al., 2006, Gleeson et al., 2009, Collins et al., 2020). Most of the previously reported conceptual models for granitic/hard rock regions related to groundwater, mainly focused on the top weathered and fracture zones (Devandal et al., 2006, Lachassagne et al., 2011, Guihéneuf et al., 2014) and barely discuss the role of blind/open sheet joints as potential aquifers at greater depths. Based on the drilling information, well construction details of studied wells, field conditions and observations, a conceptual model (Fig. 9) is proposed to understand the groundwater dynamics in the present study area.

The large variations observed in hydrochemistry and stable isotope values for the shallow (60 to 100 m) and deep (~400 m) wells waters clearly indicate that the respective aquifers were not communicating in the absence of connecting vertical joints/fractures and hence, the deep aquifer was under confined like condition. Drilling information of 5 deep wells shows that, for all the wells, an aquifer was encountered almost at the same depth (~ >360 m) after crossing the hard and compact granite, thereby implying the existence of deep aquifer in this area. Low ^{14}C activity in the deep groundwater (long residence time) specifies stagnation/long flow paths of groundwater in the discrete/blind sheet joints. Sudden change in hydrochemistry and stable isotope values only in D1 well water (~ 300 m east of granite quarry), merely a day after the summer rainstorm event, subsequent to a prolonged drought, indicates fast migration of fresh water from the nearby surface water body to the phreatic aquifer and further to the deep aquifer. Fast migration of freshwater to deep aquifer is possible only by transfer through the bore well holes which connect the phreatic and the deeper aquifer. Field observations in the granite quarry show a few sheet joints dipping towards east, which might be connected to the phreatic aquifer. When there was no water in the phreatic aquifer due to severe drought during 2014, the deep groundwater (paleo-water) was being exploited. This probably led to drastic reduction in quantum of the paleo-groundwater in the deep aquifer, which got replenished with fresh water during the high rainfall year (2016) and continued up to 2019, as evidenced from the hydrochemical and isotopic data of this study. This data complemented by the longer residence time for the three deep well waters (D1, D2 and D3) from January 2015 to June 2016 are interpreted in terms of entrapment/long flow paths to the deep fracture system, where the aquifer is under confined like condition. Such a confinement within the solid granite could be possible, provided there are no or limited vertical joints crosscutting the deep and shallow aquifers. As long as the entrapped groundwater is under confined like condition, probability of the recent recharge to the deep aquifer stands minimal. Initiation of groundwater extraction from this deep aquifer in 2014 turned into over-exploitation by 2015 through drilling of additional deep wells due to which, the aquifer with limited potential was de-saturated during the drought conditions in 2014 and 2015. During the high rainfall conditions (2016) initially, the shallow aquifer replenished with (i) fresh groundwater through natural rainfall recharge (ii) induced recharge through fracture network from granite quarry as well as (iii) from surrounding surface reservoirs. Once the deep aquifer got connected with the shallow one through several deep well holes, initially a part of the recharged water to shallow aquifer migrated to deep aquifer. Upon saturation of the deep aquifer, water levels in the shallow aquifer would rise. In such a scenario, the deep aquifer sustains owing to their communications and receiving induced recharge from the shallow aquifer.

Conclusion

Distinct hydrochemical and isotopic characters of the studied groundwater samples from shallow and deep aquifers in a granitic terrain show that the two-aquifer systems are not initially inter-connected. The present study indicates that, extraction of the groundwater from the limited potential deep aquifers in a way facilitates their quick replenish/replenishment by absorbing more freshwater through connecting bore holes during the high rainfall years. This further suggests that exploitation of deep groundwater, particularly in semi-arid hard rock regions could help in meeting water demands during the draught periods as

well as lead to enhancing the groundwater recharge. Also, studies on water quality of shallow aquifers and deep aquifers may provide details on water quality issues related to this interconnectivity phenomenon. Thus, the exploitation of deep aquifer system enhances groundwater recharge during the high rainfall years due to higher storage capacity created during drought years.

Declarations

ACKNOWLEDGEMENTS

The authors are grateful to the Director, CSIR - National Geophysical Research Institute for kind support and encouragement to carry out this work. The authors profoundly thank the technical staff of the ^{14}C laboratory for their help in the sample collection and processing. Special thanks to Dr. B.S. Sukhija, Ex scientist G, CSIR-NGRI for his time to time discussions and advice on the subject. We also thank Dr. P. Mudanure, Director State Groundwater Department, Telangana for providing the groundwater levels close to study area.

References

1. Ayraud V, Aquilina L, Labasque T, Pauwels H, Molenat J, et al (2008) Compartmentalization of physical and chemical properties in hard-rock aquifers deduced from chemical and groundwater age analysis. *Applied Geochemistry*, 23(9) 2686-2707. <10.1016/j.apgeochem.2008.06.001> <insu-00338893>
2. Bahat D, Grossenbacher K, Karasaki K (1995). Investigation of Exfoliation Joints in Navajo Sandstone at the Zion National Park and in Granite at the Yosemite National Park by Tectonofractographic Techniques. Berkeley
3. BIS (2012) Bureau of Indian Standards specification for drinking water. 2nd revision of IS: 10500:2012. Bureau of Indian Standards, New Delhi.
4. CGWB (2011) Ground water scenario in major cities of India, Report of Central Ground Water Board, Ministry of water resources, India. pp 239
5. CGWB (2016) Groundwater year Book 2025-16, Telangana State. Report of Central Ground Water Board, Ministry of water resources, India. pp 90.
6. Chandra S, Nagaiah E, Reddy DV, Rao AV, Ahmed S (2012) Exploring deep potential aquifer in water scarce crystalline rocks. *Journal of Earth System Science*, 121(6), 1455–1468.
7. Chandra S, Auken E, Maurya PK, Ahmed, SA, Verma SK (2019) Large Scale Mapping of Fractures and Groundwater Pathways in Crystalline Hardrock By AEM. *Scientific Reports*, 9, 398. DOI:10.1038/s41598-018-36153-1
8. Collins SL, Loveless SE, Muddu S, Buvaneshwari S (2020) Groundwater connectivity of a sheared gneiss aquifer in the Cauvery River basin, India. *Hydrogeology Journal*, 28, 1371–1388. <https://doi.org/10.1007/s10040-020-02140-y>
9. Cook PG (2000) A guide to regional groundwater flow in fractured rock aquifers, Seaview Press: Henley Beach, South Australia, 108pp
10. Cook PG, Love AJ, Robinson NI, Simmons CT (2005) Groundwater ages in fractured rock aquifers. *Journal of Hydrology* 308, 284–301.
11. Craig H, (1961) Isotopic variation in meteoric water. *Science*, 133, 1702-1703.
12. Dewandel B, Lachassagne P, Wyns R, Maréchal JC, Krishnamurthy NS (2006) A generalized 3-D geological and hydrogeological conceptual model of granite aquifers controlled by single or multiphase weathering. *Journal of Hydrology*, 330(1-2), 260-284.
13. Durand V, Léonardi V, de Marsily G, Lachassagne P (2017) Quantification of the specific yield in a two-layer hard-rock aquifer model. *Journal of Hydrology*, 551, 328–339.
14. de Graaf Inge EM, Gleeson T, (Rens) van Beek LPH, Sutanudjaja EH, Bierkens MFP (2019) Environmental flow limits to global groundwater pumping. *Nature*, 574, 90-94.
15. Gleeson T, Novakowski K, Kurt Kyser T (2009) Extremely rapid and localized recharge to a fractured rock aquifer. *Journal of Hydrology*, 376, 496–509.
16. Guihéneuf N, Boisson A, Bour O, Dewandel B, Perrin J, Dausse A (2014) Groundwater flows in weathered crystalline rocks: Impact of piezometric variations and depth-dependent fracture connectivity. *Journal of Hydrology*, 511, 320–324.
17. Gupta SK, Polach H (1985) Radiocarbon dating practices at ANU. Radiocarbon lab Res School of Pac. Studies, Australian National University, Canberra, p 176
18. He J, Ma J, Zhang P, Tian L, Zhu G, Edmunds WM (2012) Groundwater recharge environments and hydrogeochemical evolution in the Jiuquan Basin, Northwest China. *Applied Geochemistry*, 27, 866-878.
19. Holzhausen GR (1977). Sheet Structure in Rock and Some Related Problems in Rock Mechanics. Stanford
20. IAEA (2013) Isotope Methods for Dating Old Groundwater, IAEA STI/PUB/1587, (2013), <https://www.iaea.org/publications/8880/isotope-methods-for-dating-old-groundwater>
21. Ian Cartwright I, Currell MJ, Cendón DI, Meredith, KT (2020) A review of the use of radiocarbon to estimate groundwater residence times in semi-arid and arid areas. *Journal of Hydrology*, 580, 124247
22. Jahns RH (1943) Sheet structure in granites: its origin and use as a measure of glacial erosion in New England. *Journal of Geology*, 51, 71-98.
23. Kumar B, Rai SP, Kumar US, Verma SK, Garg P, Kumar SV, Pande NG (2010) Isotopic characteristics of Indian precipitation. *Water Resources Research*, 46(12).
24. Lachassagne P, Wyns R, Dewandel B (2011) The fracture permeability of Hard Rock Aquifers is due neither to tectonics, nor to unloading, but to weathering processes. *Terra Nova*, 23(3), 145–161. DOI: 10.1111/j.1365-3121.2011.00998.x
25. Liang-Feng Han LF, Leonard I, Wassenaar LI (2021) Principles and uncertainties of ^{14}C age estimations for groundwater transport and resource evaluation. *Isotopes in Environmental and Health Studies* 57, 111-141. <https://doi.org/10.1080/10256016.2020.1857378>

26. Maheshwari K, Senthil Kumar P, Mysaiah D, Ratnamala K, Sri Hri Rao M, Seshunarayana T (2013) Ground Penetrating Radar for Groundwater Exploration in Granitic Terrains: A Case Study from Hyderabad. *Journal Geological Society of India*, 81, 781-790.
27. Martel SJ (2017) Progress in understanding sheeting joints over the past two centuries. *Journal of Structural Geology*, 94, 68-86.
28. Matthes FE (1930) *Geologic History of the Yosemite Valley*.
29. Ofterdinger U, MacDonald AM, Comte J.-C, Young ME (2019) Groundwater in fractured bedrock environments: managing catchment and subsurface resources – an introduction. Geological Society, London. Special Publications, 479, 1-9. <https://doi.org/10.1144/SP479-2018-170>
30. Piper AM (1944) A graphic procedure in the geochemical interpretation of water analyses. *Am Geophys Union Trans*, 25:914–923.
31. Ray RK, Mukherjee R (2008) Hydrochemical evaluation of groundwater in the phreatic aquifers of Chhattisgarh. *Journal of geological Society of India* 72, 405-414.
32. Reddy DV, Nagabhushanam P, Sukhija BS, Reddy AGS (2009) Understanding hydrological processes in a highly stressed granitic aquifer in southern India. *Hydrological Processes*, 23, 1282–1294.
33. Reddy DV, Nagabhushanam P, Edward Peters (2010) Village environs as source of nitrate contamination in groundwater: A case study in basaltic geoenvironment in central India. *Environmental Monitoring and Assessment*, 174, 481-492.
34. Reddy DV, Nagabhushanam P, Madhav T, Chandrakala P, Reddy AGS (2015) Characterization of groundwater contaminant sources in the coastal sand dune aquifer, Prakasham district, A.P. India. *Environmental Earth Science*, 74, 3453-3466.
35. Roy A, Keesari T, Pant D, Rai G, Sinha UK, Mohokar H, Iyarl A, Sharma DA (2021). Unravelling 30 Ka recharge history of an intensively exploited multi-tier aquifer system in North West India through isotopic tracers – Implications on deep groundwater sustainability. *Science of The Total Environment* DOI:10.1016/j.scitotenv.2021.151401
36. Singhal BBS, Gupta RP (1999) Fractures and discontinuities. In: *Applied Hydrogeology of Fractured Rocks*. Springer, Dordrecht
37. Sreedevi PD, Ahmed S, Reddy DV (2017) Mechanism of Fluoride and Nitrate Enrichment in Hard-Rock Aquifers in Gooty Mandal, South India. *Environ. Process*, 4:625–644. DOI 10.1007/s40710-017-0254-7
38. Stephen J (2010). Martel Progress in understanding sheeting joints over the past two centuries. *Journal of Structural Geology*, 94, 68-86.
39. Stuiver M, Pollach HA (1977) Discussion reporting of ¹⁴C data. *Radiocarbon*, 19(3), 355-363.
40. Sukhija BS, Reddy DV, Nagabhushanam P, Bhattacharya SK, Jani RA, Kumar D (2006). Characterisation of recharge processes and groundwater flow mechanisms in weathered-fractured granites of Hyderabad (India) using isotopes. *Hydrogeology Journal*, 14, 663-674.
41. Takahashi HA, Nakamura T, Tsukamoto H, Kazahaya K, Handa H, Hirota A (2013) Radiocarbon dating of groundwater in Granite Fractures in Abukuma Province, Northeast Japan. *Radiocarbon*, 55 (2): Proc. of the 21st International Radiocarbon Conference (Part 1 of 2), 894 – 904. DOI: <https://doi.org/10.1017/S0033822200058057>
42. Wakode HB, Baier K, Jha R, Azzam R (2014). Analysis of urban growth using Landsat TM/ETM data and GIS—a case study of Hyderabad, India. *Arabian Journal of Geosciences*, 7, 109–121.
43. WHO (2008) Guidelines for drinking-water quality—Incorporating first addendum to Third Edition. Recommendations (Vol. 1, p. 595). Geneva. http://www.who.int/water_sanitation_health/dwq/GDWPrecomdrev1and2.pdf.

Tables

Table 1. Sampling details for hydrochemical and isotopic measurements

Sample ID	Depth (m)	2015		2016		2017		2019	
		Che*	¹⁴ C	Che*	¹⁴ C	Che*	Che*	Che*	¹⁴ C
D1 (deep)	396	9	3	7	3	1	1	2	1
D2 (deep)	396	8	3	7	3	1	1	2	1
D3 (deep)	390	3	2	4	3	1	1	2	1
D4 and D5 (Surrounding deep wells)	410	2							
	397								
S1 to S4 (Surrounding shallow wells)	61 to 107	4							
QS (Quarry sample)								1	

Table 2 Statistical distribution of hydrochemical parameters of all collected samples, one-time collection from shallow wells and repeated sampling from the deep wells.

	pH	Eh	Cond	TDS	Na	K	Mg	Ca	Cl	SO ₄	HCO ₃	NO ₃	F	Br	¹⁸ O	D
		mV	uS/cm	mg/L	mg/L	mg/L	mg/L	mg/L	‰	‰						
Total samples																
Average	7.25	-50	1816	1271	202	5	21	224	473	209	174	39.6	2.3	1.5	-1.70	-15.42
Minimum	6.13	-103	717	502	29	1	11	66	70	52	50	0.0	0.0	0.0	-6.25	-46.95
Maximum	7.94	1	2760	1932	334	23	30	361	1048	480	320	162	3.6	5.4	8.28	27.69
Stand deviation	0.34	26	551	386	88	4	5	85	319	92	101	48.0	0.6	1.6	2.13	9.29
Deep wells																
Average	7.44	-79	1973	1381	240	6	17	231	566	214	100	0.0	2.5	1.5	-2.33	-17.19
Minimum	7.35	-85	1370	959	169	4	11	143	310	148	70	0.0	2.2	0.0	-2.49	-18.76
Maximum	7.55	-76	2660	1862	323	8	24	350	870	280	150	0.0	2.8	2.5	-1.89	-14.70
Stand deviation	0.08	4	538	377	64	2	5	88	237	55	36	0.0	0.3	1.1	0.29	1.74
Shallow wells																
Average	6.46	-25	937	656	55	1	25	121	98	71	263	62.9	2.4	0.0	0.79	-3.59
Minimum	6.13	-40	717	502	29	1	22	74	70	52	230	32.0	1.8	0.0	-2.39	-18.75
Maximum	6.74	-7	1200	840	78	2	30	177	128	92	300	125	2.7	0.0	8.28	27.69
Stand deviation	0.30	15	250	175	24	0	4	43	32	21	29	42.7	0.4	0.0	5.03	21.16
Quarry sample																
30/08/2019	7.85	-55	4440	3108	536	456	100	254	933	711	565	0.0	0.0	n.a	2.04	7.77

Table 3 Water type, hydrochemistry, stable isotopic values and carbon-14 activity of collected samples from study area

well	depth	Sampling	groundwater	pH	Eh	Cond	TDS	Na	K	Mg	Ca	Cl	SO ₄	HCO ₃	NO ₃	F
id	m	date	type		mV	uS/cm	mg/L	mg/L	mg/L	mg/						
D1	396	12-01-15	Ca-Na-Cl	7.55	-84	2320	1624	280	3	19	287	761	245	60	1.6	2.5
		03-02-15	Ca-Na-Cl	7.25	-67	2380	1666	286	4	21	293	788	246	50	0.0	2.1
		11-02-15	Ca-Na-Cl	7.15	-62	2460	1722	311	3	22	301	849	264	50	0.0	2.4
		10-04-15	Ca-Na-Cl	7.42	-78	2660	1862	323	4	24	350	870	280	70	0.0	2.4
		16-04-15	Ca-Na-Cl-HCO ₃	6.72	-40	1510	1057	136	13	24	208	224	153	260	133.3	1.2
		21-04-15	Ca-Na-Cl	7.10	-60	2510	1757	312	5	25	323	794	274	70	8.0	2.2
		05-05-15	Ca-Na-Cl	7.05	-57	2630	1841	322	5	27	337	874	279	60	8.0	3.0
		12-07-15	Ca-Na-Cl	7.79	-97	2590	1813	307	4	26	333	843	278	70	12.7	2.6
		04-09-15	Ca-Na-Cl	7.40	-76	2760	1932	334	4	27	361	906	302	60	2.8	2.2
		01-01-16	Ca-Na-Cl-SO ₄	7.48	-40	2540	1778	302	3	26	352	1030	343	80	2.8	3.6
		06-01-16	Ca-Na-Cl-SO ₄	7.24	-28	2450	1715	293	4	27	347	993	339	90	11.3	2.9
		25-05-16	Ca-Na-Cl-SO ₄	7.36	-42	2440	1708	318	4	24	321	815	307	70	0.0	2.2
		07-06-16	Ca-Na-Cl-SO ₄	7.53	-51	2440	1708	313	3	24	317	818	302	70	0.0	2.0
		26-09-16	Ca-Na-SO ₄ -Cl	7.36	-43	1440	1008	138	18	20	236	185	355	160	162.1	0.9
		15-12-16	Ca-Na-HCO ₃ -Cl	6.92	-19	1380	966	119	4	26	149	158	114	300	110.6	2.5
22-12-16	Ca-Na-HCO ₃ -Cl	7.08	-26	1390	973	129	3	20	160	175	113	320	84.6	2.4		
02-04-17	Ca-Na-Cl-HCO ₃	6.90	-22	1530	1071	120	4	27	180	196	137	300	146.1	2.4		
20-01-18	Na-Ca-HCO ₃ -Cl	6.94	-55	1200	840	109	2	22	66	125	86	310	75.0	2.1		
27-03-19	Ca-Na-Cl-HCO ₃	6.90	1	1580	1106	130	3	19	209	263	141	265	47.3	2.6		
30-08-19	Ca-Na-HCO ₃ -Cl	6.90	-5	1290	903	107	2	17	162	152	110	295	60.4	2.7		
D2	396	12-01-15	Ca-Na-Cl-SO ₄	7.61	-87	1730	1211	213	5	14	201	479	202	100	1.4	2.6
		03-02-15	Ca-Na-Cl-SO ₄	7.28	-70	1670	1169	208	5	14	186	467	194	100	0.0	2.8
		11-02-15	Ca-Na-Cl-SO ₄	7.28	-71	1670	1169	202	5	14	183	462	195	110	0.0	2.6
		10-04-15	Ca-Na-Cl	7.55	-85	2050	1435	247	4	17	235	608	225	80	0.0	2.2
		16-04-15	Na-Ca-Cl-SO ₄	7.28	-71	1580	1106	200	6	13	169	407	174	120	0.0	2.3
		28-04-15	Ca-Na-Cl-SO ₄	7.32	-71	1890	1323	233	5	16	207	499	206	90	4.8	2.4
		12-07-15	Ca-Na-Cl	7.72	-94	2570	1799	301	4	23	314	843	280	80	7.7	2.5
		02-09-15	Ca-Na-Cl	7.94	-103	2660	1862	325	4	25	348	873	291	70	0.0	2.3
		01-01-16	Ca-Na-Cl-SO ₄	7.50	-41	2410	1687	286	4	25	338	986	341	100	3.2	2.9
		08-01-16	Ca-Na-Cl-SO ₄	7.50	-41	2490	1743	306	3	26	357	1048	355	80	2.6	2.7

		25-05-16	Ca-Na-Cl-SO4	7.53	-52	2450	1715	311	3	23	312	857	320	70	0.0	2.5
		08-06-16	Ca-Na-Cl-SO4	7.57	-53	2430	1701	314	3	24	313	820	310	80	0.0	2.3
		26-09-16	Ca-Na-SO4-Cl	7.52	-51	1630	1141	137	23	23	278	178	480	220	130.4	0.4
		15-12-16	Ca-Na-Cl-HCO3	7.15	-30	1430	1001	143	5	20	144	192	135	310	88.9	2.1
		22-12-16	Ca-Na-Cl-HCO3	7.10	-28	1420	994	143	5	20	167	195	132	310	82.0	2.3
		02-04-17	Ca-Na-Cl-HCO3	7.02	-26	1530	1071	121	3	26	208	193	130	310	137.2	2.1
		20-01-18	Na-Ca-HCO3-Cl	7.03	-60	1240	868	120	3	21	73	131	94	315	70.3	2.3
		27-03-19	Ca-Na-Cl-SO4-HCO3	7.15	-16	1540	1078	127	3	19	203	258	227	275	47.3	0.0
		30-08-19	Ca-Na-HCO3-Cl-SO4	7.29	-25	1190	833	128	9	12	128	147	122	255	37.3	2.2
D3	390	10-04-15	Na-Ca-Cl-SO4	7.42	-78	1370	959	169	7	11	143	310	148	150	0.0	2.5
		22-05-15	Ca-Na-Cl-SO4	7.63	-88	1290	903	150	9	13	154	247	168	170	37.7	1.8
		02-09-15	Ca-Na-Cl-SO4	7.80	-97	1870	1309	221	7	17	225	508	217	120	7.6	2.7
		08-01-16	Ca-Na-Cl-SO4	7.54	-43	1900	1330	227	6	18	247	707	277	120	7.6	3.4
		13-06-16	Ca-Na-Cl-SO4	7.50	-49	1950	1365	255	4	19	233	568	234	130	0.7	2.3
		15-12-16	Ca-Na-Cl-HCO3-SO4	7.18	-32	1410	987	139	8	21	138	182	151	290	78.9	1.9
		22-12-16	Ca-Na-Cl-HCO3-SO4	7.11	-28	1410	987	139	8	21	156	186	155	290	81.9	2.2
		02-04-17	Ca-Na-Cl-HCO3	7.14	-33	1520	1064	134	4	25	202	211	141	290	125.8	2.6
		20-01-18	Na-Ca-HCO3-Cl-SO4	7.13	-64	1270	889	130	9	18	72	146	126	300	57.5	1.4
		27-03-19	Ca-Na-Cl-HCO3	7.18	-18	1530	1071	131	3	18	203	246	150	280	43.4	2.4
		30-08-19	Ca-Na-Cl-HCO3	7.28	-24	1290	903	123	4	16	155	169	125	280	45.1	2.8
D4	410	28-04-15	Ca-Na-Cl	7.27	-70	2230	1561	275	3	18	255	686	232	80	0.0	2.8
D5	397	10-04-15	Ca-Na-Cl-SO4	7.35	-76	1810	1267	223	8	15	196	475	202	100	0.0	2.8
S1	107	10-04-15	Ca-Na-Mg-HCO3-Cl	6.30	-18	1100	770	78	2	25	74	128	86	260	54.9	1.8
S2	92	10-04-15	Ca-Mg-Na-HCO3-Cl	6.13	-7	717	501.9	39	1	22	110	70	56	230	39.4	2.7
S3	92	10-04-15	Ca-Mg-HCO3-Cl	6.74	-40	730	511	29	1	22	123	70	52	260	32.0	2.7
S4	61	10-04-15	Ca-Na-HCO3-Cl	6.68	-36	1200	840	72	2	30	177	124	92	300	125.2	2.2
GQ		30-08-19	Na-Ca-K-Cl	7.85	-55	4440	3108	536	456	100	254	933	711	565	0.0	0.0

D1 - Shivam-1, D2 – Shivam-2, D3 – Shivam3, D4- Shrasta Apt., D5 – Krishna Apt., S1 – GK Siddeshwar Apt., S2 – Habib Apt., S3 – LN Villa Apt., S4 – Viniyard, GQ – Granite quarry

Figures

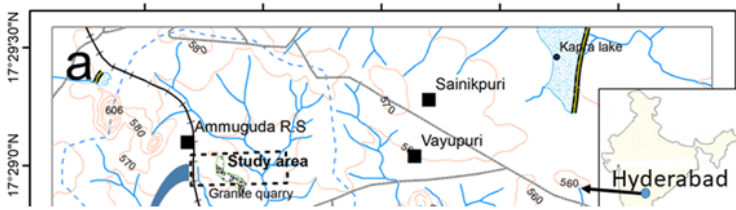


Figure 1

a Location of study area and its surroundings with drainage network, 1b. (Google Earth, imagery dated 27/5/2016) groundwater sampled wells (D - deep well and S - shallow well) with their respective numbers and the granite quarry (surface water pond) in the west is shown.

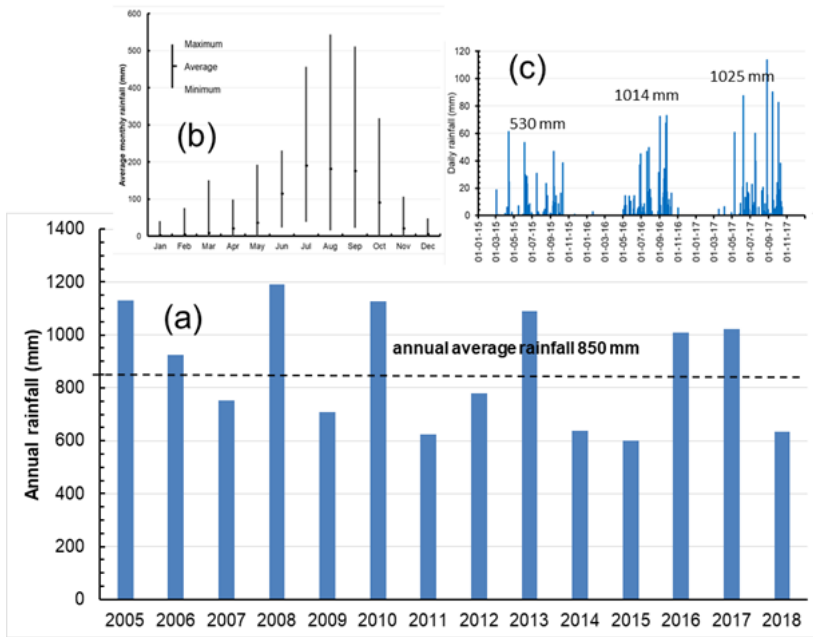


Figure 2
 a. Distribution of annual rainfall from 2005 to 2018 in the study area (b) average monthly rainfall and (c) distribution of daily rainfall during 2015 to 2017.

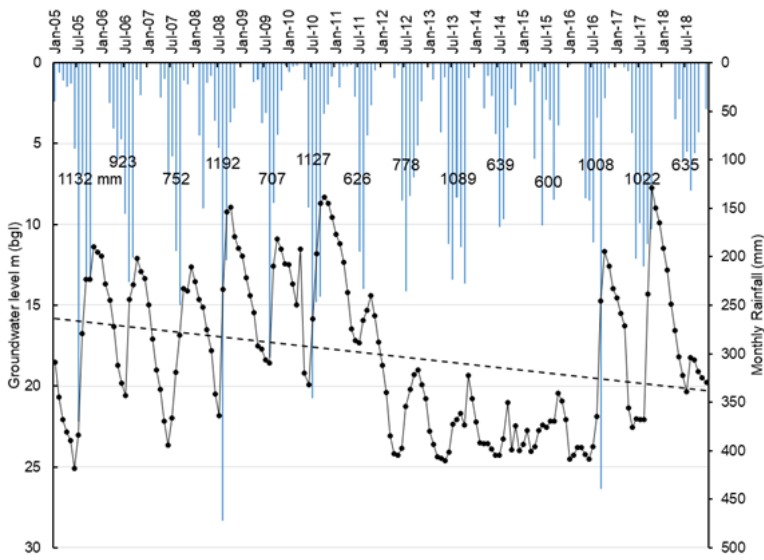


Figure 3
 Change in groundwater level with reference to rainfall (Total annual rainfall is shown in numbers (monthly groundwater levels monitored at Malkajgiri piezometer, about 3 km south of study area).

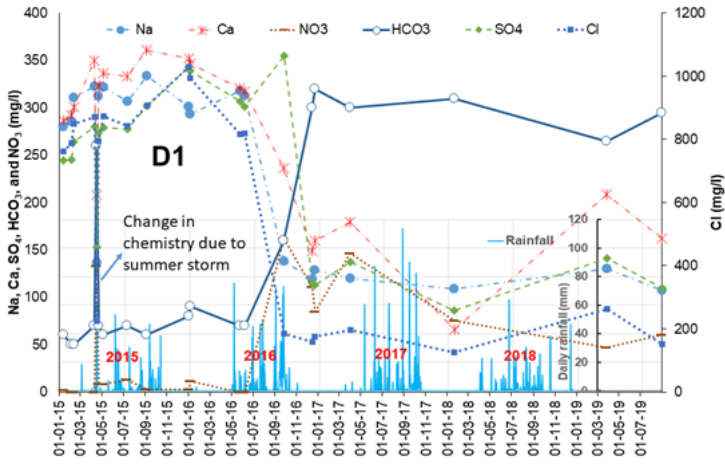


Figure 4

Temporal variation of different ions in well D1 groundwater. (increase in HCO₃ and NO₃ concentrations seen when other ions decreased)

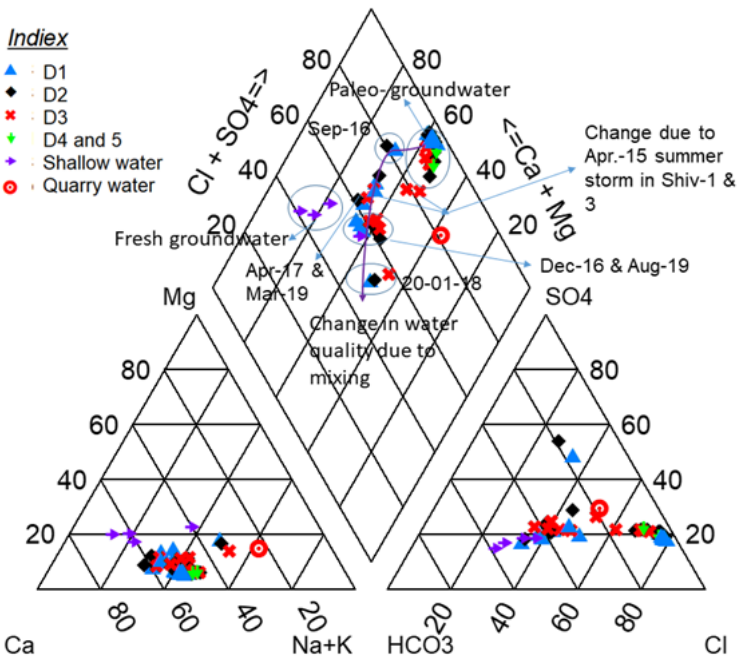


Figure 5

Water quality (facies) variation between shallow and deep groundwater and temporal variation in deep groundwater (Piper, 1944) .

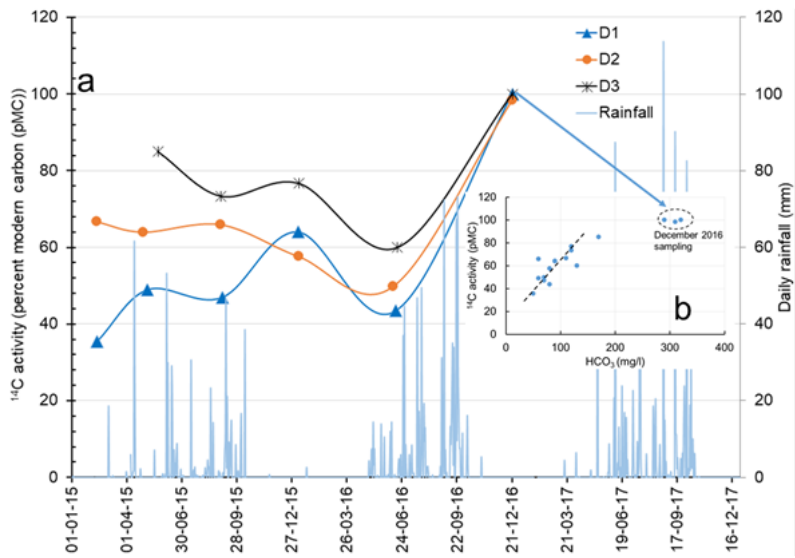


Figure 6
 a. Temporal variation of the ^{14}C activity in the 3 studied deep well waters. Daily rainfall during the study period also plotted, 8b. Relation between HCO_3^- concentration and ^{14}C activity in the deep groundwater.

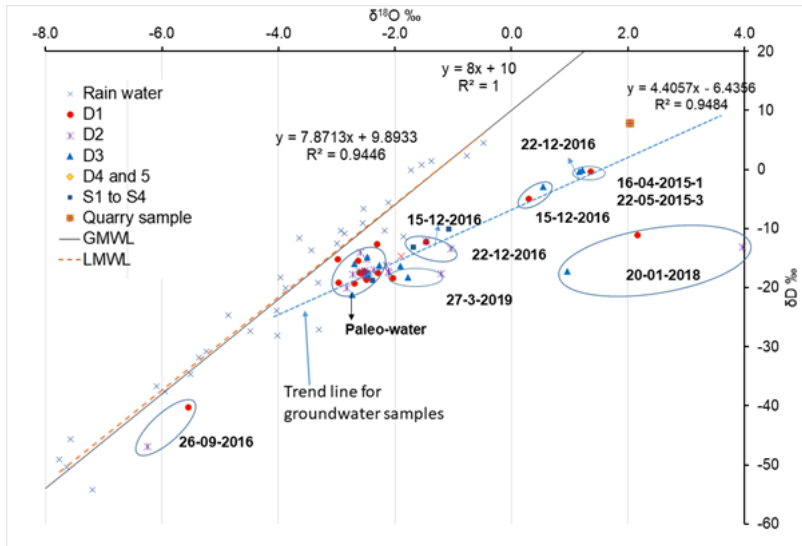


Figure 7
 $\delta^{18}\text{O}$ and δD of groundwater collected from the wells in the study area and rainwater samples from CSIR-NGRI for the year 2010.

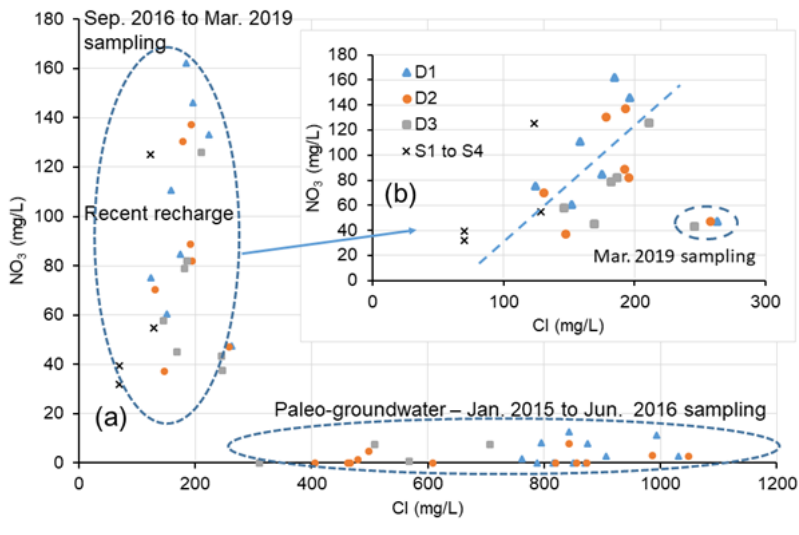


Figure 8
 a Relation between Cl and NO₃. Shallow groundwater samples collected during April 2015 and deep samples collected between September 2016 and August 2019 representing as one group, and the deep groundwater collected during January 2015 to June 2016 as another group. 8b. enlarged portion of first group, where recent recharge exists.

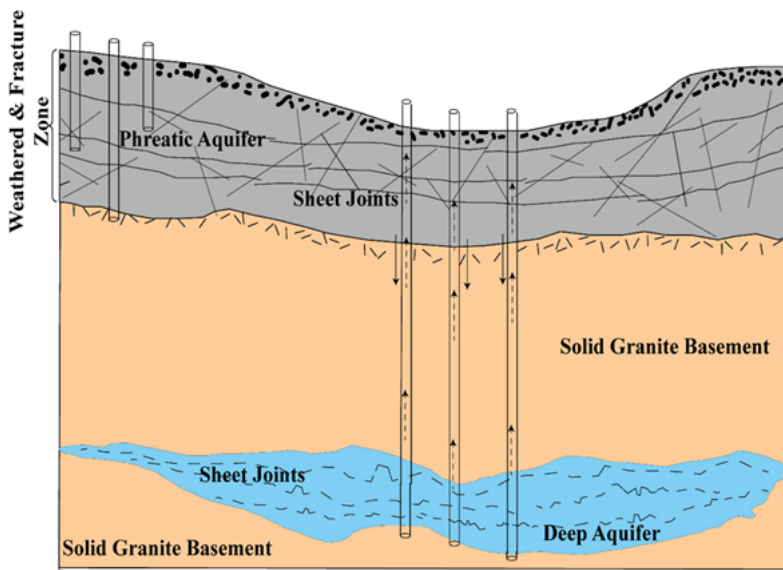


Figure 9
 A conceptual model of the granitic terrain with 3 aquifer system. Top weathered zone can be considered as phreatic aquifer, fractured zone is either phreatic/semiconfined like conditions. Sheet joint at deeper depth either blind or connected to a distant place considered as confined like aquifer. Lack of vertical fractures, the deep aquifer has no connectivity with shallow aquifer. However, connection made between the aquifers by drilling the holes for exploitation. When enough groundwater exists in the phreatic aquifer, it serves the requirement, however, when it exhausts, the deep aquifer provides as an alternate (during drought conditions) and it replenishes during the high rainfall period by induced recharge.

Supplementary Files

This is a list of supplementary files associated with this preprint. Click to download.

- [SIFig.1.tif](#)
- [SIFig.2.tif](#)